

BBP Phase Transition for an Extensive Number of Outliers

Niklas Forner,¹ Alexander Maloney,^{2,3,4} and Bernd Rosenow¹

¹*Institut für Theoretische Physik, Universität Leipzig, D-04103, Leipzig, Germany*

²*Department of Physics, Syracuse University, New York, USA*

³*Institute for Quantum & Information Sciences, Syracuse University, New York, USA*

⁴*Department of Physics, McGill University, Montréal, Canada*

Random-matrix theory helps disentangle signal from noise in large data sets. We analyze rectangular $p \times q$ matrices $W = W_0 + M$ in which the noise M generates a Marchenko–Pastur bulk, whereas the signal W_0 injects an extensive set of degenerate singular values. Keeping rank W_0/q finite as $p, q \rightarrow \infty$, we show that the singular value density obeys a quartic equation and derive explicit asymptotics in the strong-signal regime. The resulting generalized Baik–Ben Arous–Péché phase diagram yields a scaling law for the critical signal strength and clarifies how a finite density of spikes reshapes the bulk edges. Numerical simulations validate the theory and illustrate its relevance for high-dimensional inference tasks.

Contemporary data analysis frequently relies on large data sets – for example, multivariate time-series measurements or the weight matrices of deep neural networks. These data are invariably contaminated by noise. Although the main goal is to uncover the underlying signal, it is equally important to understand how noise acts on that signal to produce the observations [1]. Noise can take many forms and may exhibit correlations between different data points, thereby modifying the relation between the latent signal and the measured data.

Random Matrix Theory (RMT) was developed to predict statistical properties – such as eigenvalue and singular-value distributions – of large matrices whose entries are random variables. The framework has found applications spanning statistical and nuclear physics,[2, 3] econophysics and finance,[4, 5] meteorology and climate science, quantum mechanics,[6] image processing,[7] wireless communications,[8] neural networks,[9] and many other fields.

The spectra of random matrices have been studied extensively, and numerous models for signal matrices perturbed by noise have been proposed, see Refs. [10, 11] for reviews. In modern applications these matrices are often rectangular, and the dominant noise is typically additive – for instance, fluctuations of weights around a training minimum. In this Letter we consider rectangular $p \times q$ “signal-plus-noise” matrices $W = W_0 + M$, where W_0 encodes the signal and M represents the noise. Whereas a square matrix is characterized by its eigenvalues, a rectangular matrix is described by the eigenvalues of $W^\top W$, i.e., by the squared singular values of W . Quantifying how noise reshapes this singular-value spectrum is essential for inferring the true signal weights in settings such as late-stage neural-network training [9]. In the “thermodynamic” limit $p, q \rightarrow \infty$ with p/q fixed the spectral density is self-averaging, in the sense that the statistical properties of a typical matrix approach those of the ensemble as a whole [11, 12]. The noise component (the “bulk”) forms a continuous density with sharp edges [13–15]. A low-rank perturbation satisfying rank $W_0/q \rightarrow 0$

does not affect the bulk but produces isolated eigenvalues. When these eigenvalues are large enough, they will separate from the continuous bulk; the point at which they emerge from the bulk is the Baik–Ben Arous–Péché (BBP) phase transition [12, 15, 16].

Here we analyze a complementary regime, an *extensive* number of outliers – i.e. a signal matrix whose rank scales linearly with p and q – whose collective effect reshapes the bulk spectrum (see Fig. 1). We will find a similar phase transition, where for sufficiently large signal an entire continuous signal distribution separates from the bulk “noise” part of the spectrum. Of course, the location of this phase transition, as well as the shape of both the bulk and the signal distributions, will depend on the properties of W_0 and M . We begin with a single deviating singular value of degeneracy r , with rank ratio $\tilde{r} := r/q$ finite in the large q limit. The full spectrum is then governed by a fourth-order algebraic equation, from which we determine the location of the phase transition and the shape of the signal and noise distributions and derive an explicit asymptotic solution at large signal strength. We map out the generalized BBP phase diagram as a function of \tilde{r} and signal strength, and uncover a scaling law relating the critical signal strength to both \tilde{r} and the aspect ratio p/q . We verify these analytical results by matching to numerical simulations. For more complicated signal distributions, with n distinct singular values, we find an analogous result where the spectrum is determined by an algebraic equation of order $2n + 2$.

In related work, Ganguli et al. [17] analyzed an extensive-rank “spike” model in the context of optimal, rotationally invariant estimators for the population covariance matrix, with further developments in Refs. [18–22]. Our analysis addresses the same regime and reproduces their principal findings within a complementary formulation, while extending them in several significant ways. First, we obtain a scaling law that relates the critical signal strength to both the rank ratio and the matrix aspect ratio. Second, we derive an explicit asymptotic expression for the signal-induced part of the spectrum,

which avoids the numerical solution of self-consistency equations and remains accurate for finite matrix sizes. Third, for signal ensembles with power-law distributed singular values, we obtain a closed analytic equation for the spectral function, allowing a detailed characterization of the corresponding population distribution.

Model: We consider a real $p \times q$ matrix expressed as a sum of signal and noise $W = W_0 + M$ with $p, q \in \mathbb{N}$. Our goal is to find the limiting singular-value density $\rho(\lambda) = 2\lambda P(\lambda^2)$, where $P(x)$ is the average eigenvalue density of $W^\top W$ in the thermodynamic limit $p, q \rightarrow \infty$ at fixed aspect ratio $\mathcal{A} := p/q$. Averages $\langle \cdot \rangle_M$ are taken with respect to the Gaussian measure

$$\langle \cdot \rangle_M = \frac{1}{(2\pi)^{pq/2}} \int_{\mathbb{R}^{pq}} \mathcal{D}M (\cdot) e^{-\frac{p}{2\sigma^2} \text{Tr}(M^\top M)} \quad (1)$$

with integration measure $\mathcal{D}M = \prod_{i=1}^p \prod_{j=1}^q dM_{ij}$. The entries M_{ij} are independently and identically drawn (i.i.d.) random variables centered around zero:

$$\langle M_{ia} \rangle_M = 0, \quad \langle M_{ia} M_{jb} \rangle_M = \frac{\sigma^2}{p} \delta_{ij} \delta_{ab}. \quad (2)$$

We introduce the Green function as the limiting average trace of the resolvent of $W^\top W$

$$G(z) := \lim_{q \rightarrow +\infty} \left\langle \frac{1}{q} \text{Tr} \left[\frac{1}{z - W^\top W} \right] \right\rangle_M \quad (3)$$

which is normalized so that the eigenvalue density is

$$P(x) = -\frac{1}{\pi} \text{Im} G(x + i0^+). \quad (4)$$

We further define the partition function Z as the following multidimensional Gaussian integral,

$$Z(z) := \frac{1}{\sqrt{\det(z - W^\top W)}} \quad (5a)$$

$$= \left(\frac{q}{2\pi} \right)^{q/2} \int_{\mathbb{R}^q} \mathcal{D}X e^{-\frac{q}{2} X^\top (z - W^\top W) X} \quad (5b)$$

with $\mathcal{D}X = \prod_{i=1}^q dX_i$, so that

$$G(z) = \lim_{q \rightarrow +\infty} \left(-\frac{2}{q} \right) \partial_z \langle \ln Z(z) \rangle_M. \quad (6)$$

We therefore need to compute the expectation value of $\ln Z(z)$ – essentially a “quenched average” – which is done using the replica trick. In particular, we compute $\langle Z^n(z) \rangle_M$ for $n \in \mathbb{N}$ and analytically continue in n to compute

$$\langle \ln Z(z) \rangle_M = \lim_{n \rightarrow 0} \frac{\langle Z^n(z) \rangle_M - 1}{n}. \quad (7)$$

As usual when using the replica trick, we rely on Carlson’s theorem (and analyticity in the large q limit) to guarantee that this procedure works.

The generalization to other setups is in many cases straightforward. For example, for complex $W \in \mathbb{C}^{p \times q}$, one has to replace the transpose by the Hermitian conjugate and modify Gaussian average and partition function to account for complex-valued integration variables. Similarly, one can also consider more complicated noise spectra where Eq. (2) is replaced by the general Gaussian moments $\langle M_{ia} \rangle_M = \bar{M}_{ia}$ and $\langle M_{ia} M_{jb} \rangle_M = C_{ij} \Sigma_{ab}$. In this case the resulting spectrum can be computed using the same techniques, but the resulting coupled equations are more complicated and must generally be studied numerically. In the following we restrict ourselves to real W with i.i.d. noise centered around zero.

Outliers for White Noise: We will begin by assuming that the signal W_0 has r non-zero singular values $\{\vartheta_i\}_{i=1,\dots,r}$. The computation follows the steps proposed by Sengupta and Mitra ([23]), extended to general noise with an added signal matrix. Details are found in the Appendix, but can be summarized as follows. The average $\langle Z^n(z) \rangle_M$ can be interpreted as the partition function of n copies of the system, and is computed by introducing certain auxiliary variables (implementing a Hubbard-Stratonovich transformation). The resulting integral has a saddle point in the thermodynamic large q limit. The corresponding saddle point has replica symmetry, in the sense that it is symmetric under the interchange of copies of the system. As a result the equations for the saddle point can be rewritten in a simple form, as a single equation for the resolvent $G(z)$:

$$G(z) = \frac{1}{z \left[1 - \frac{\sigma^2}{\mathcal{A}} G(z) \right] - \sigma^2 \left(1 - \frac{1}{\mathcal{A}} \right)} \left(1 + \lim_{q \rightarrow +\infty} \frac{1}{q} \times \sum_{i=1}^r \frac{\vartheta_i^2}{\left[1 - \frac{\sigma^2}{\mathcal{A}} G(z) \right] \left(z \left[1 - \frac{\sigma^2}{\mathcal{A}} G(z) \right] - \sigma^2 \left(1 - \frac{1}{\mathcal{A}} \right) \right) - \vartheta_i^2} \right) \quad (8)$$

To understand this, first consider the case where r remains finite in the large q limit. Then the second line of equation (8) vanishes for generic values of z , leaving us with a quadratic equation for $G(z)$ whose solution is

$$G_{\pm}^{\text{MP}}(z) = \frac{\mathcal{A}}{2\sigma^2 z} \left[z - \sigma^2 \left(1 - 1/\mathcal{A} \right) \pm \sqrt{[z - \sigma^2 \left(1 + 1/\mathcal{A} \right)]^2 - 4\sigma^4/\mathcal{A}} \right]. \quad (9)$$

This is precisely the resolvent of the Marchenko-Pastur distribution, which reflects the fact that in the large q limit a finite number of signal eigenvalues will not alter the “bulk” noise part of the spectrum. At particular values of z , however, the denominator in the second line of equation (8) vanishes and $G(z)$ diverges; this indicates the existence of an outlying single eigenvalue that emerges from the bulk. The location of these divergences is found by setting $G = G_{-}^{\text{MP}}$, which reproduces the usual BBP phase transition. We conclude that in this case the

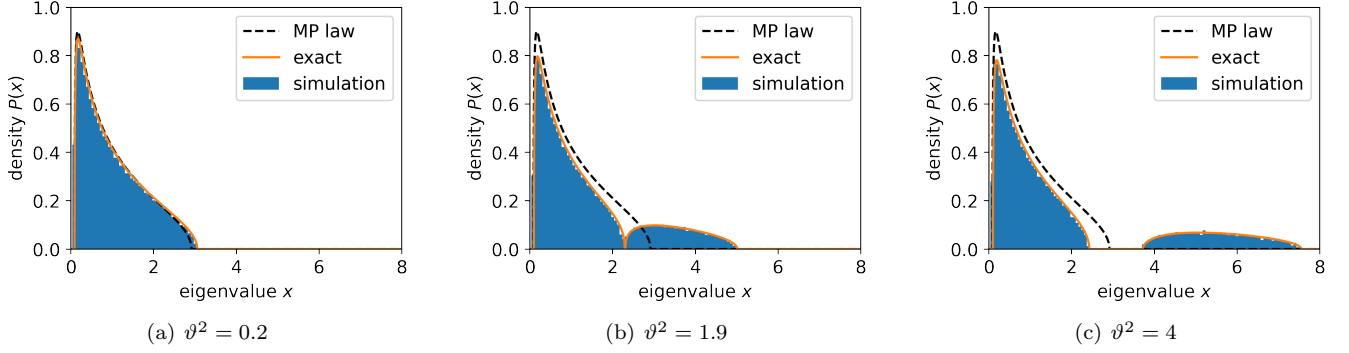


FIG. 1. Splitting of the spectrum for increasing signals at a fixed rank ratio. $\sigma = 1$, $\mathcal{A} = 2$, $\tilde{r} = 0.2$. The simulations for the spectrum of $W^\top W$ are conducted for $p \times q$ matrices $W = M + W_0$ with $p = \mathcal{A}q$ and $q = 1000$, averaged over a number of ten runs. Each entry in M is drawn from a centered normal distribution with unit variance. The Marchenko-Pastur (MP) law acts as a reference for the noise-only case.

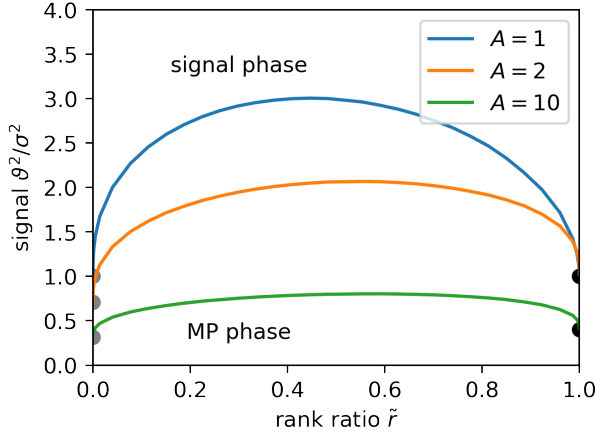


FIG. 2. Phase diagram for $\mathcal{A} \in \{1, 2, 10\}$, $\sigma = 1$. In the MP (Marchenko-Pastur) phase the spectrum exhibits one bulk, in the signal phase two – the noise and signal bulk. Numerical procedure: for a fixed \tilde{r} , the signal is increased until the discriminant of Eq. (8), see Appendix, no longer gives two but four roots (or three at the exact phase transition). Each root corresponds to a boundary of the spectrum.

largest r eigenvalues of $W^\top W$ are given by

$$x_i = \begin{cases} \frac{(\vartheta_i^2 + \sigma^2)(\vartheta_i^2 + \sigma^2/\mathcal{A})}{\vartheta_i^2}, & \vartheta_i^2 \geq \sigma^2 \mathcal{A}^{-1/2} \\ \sigma^2 (1 + 1/\sqrt{\mathcal{A}})^2, & \text{else} \end{cases} \quad (10)$$

in the large q limit. This reproduces a special case explored by Benaych-Georges and Nadakuditi ([12]), which we now see is valid for any W_0 . Hoyle and Rattray ([24] [25]) also found this relation using a similar model and similar methods.

When r scales linearly with q , however, the second line of (8) is order one for generic values of z and the spectrum is no longer Marchenko-Pastur. The easiest case is when W_0 has an r -fold degenerate singular value ϑ , with $\tilde{r} = r/q$ fixed. We can then write the self-consistency

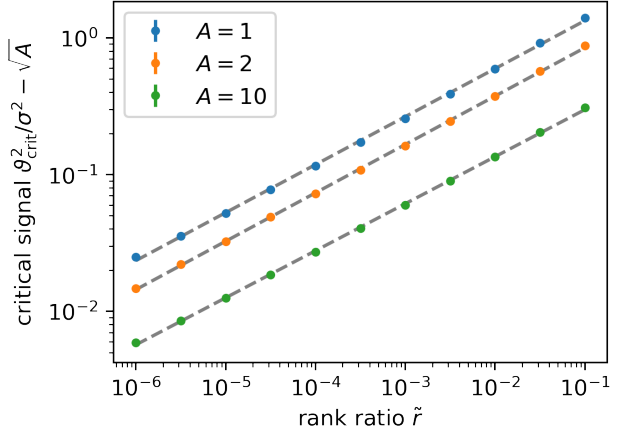


FIG. 3. A zoom-in on the low-rank regime. By subtracting $\sigma^2/\sqrt{\mathcal{A}}$ from the critical signals, we reveal the convergence to the BBP phase transition in the limit $\tilde{r} \rightarrow 0$ with a uniform scaling. The dashed lines are fits with rounded slopes 0.35, 0.35, and 0.34 for $\mathcal{A} \in \{1, 2, 10\}$ with rounded multiplicative constants $3.0 \cdot \mathcal{A}^{-0.66}$. This suggests the scaling law $3\mathcal{A}^{-2/3} \tilde{r}^{1/3}$.

equation as

$$\begin{aligned} & -\frac{z\sigma^2}{\mathcal{A}} [G(z) - G_-^{\text{MP}}(z)] [G(z) - G_+^{\text{MP}}(z)] \\ & = \frac{\tilde{r}\vartheta^2}{[1 - \frac{\sigma^2}{\mathcal{A}} G(z)] (z[1 - \frac{\sigma^2}{\mathcal{A}} G(z)] - \sigma^2 (1 - \frac{1}{\mathcal{A}})) - \vartheta^2} \end{aligned} \quad (11)$$

displaying the influences of noise (left-hand side) and signal (right-hand side). This is a fourth-order polynomial in $G(z)$ which can be solved exactly; see Appendix. Only one of these four solutions has non-negative density of states, allowing us to determine the spectrum analytically.

In Fig. 1, we show the corresponding density for several

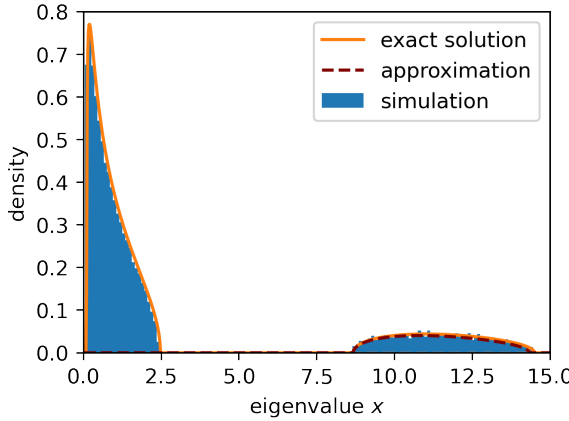


FIG. 4. Approximate spectral density by Eq. (14) in comparison with the exact spectrum and simulations for a $q = 500$ matrix averaged over 10 runs. $\mathcal{A} = 2$, $\sigma = 1$, $\tilde{r} = 0.2$, $\vartheta^2 = 10$.

signal strengths, compare it to the Marchenko-Pastur law, and confirm the distribution with numerical simulations. As the rank ratio \tilde{r} decreases, the bulk part of the spectrum approaches Marchenko-Pastur law. As the signal θ is increased the spectrum splits into two parts, with a fraction $1 - \tilde{r}$ of the eigenvalues forming a bulk similar to Marchenko-Pastur, and the remaining eigenvalues forming a continuous “signal” part of the distribution. The critical value of the signal at which this separation occurs marks a phase boundary, and is our generalization of the BPP phase transition to signals of large rank.

This behavior – the emergence of signal distribution at a critical value of θ – can be found for every rank ratio \tilde{r} . As a result, we obtain the phase diagram Fig. 2 as θ and \tilde{r} are varied. The Marchenko-Pastur (MP) phase is characterized by a single bulk, the signal phase by two disconnected parts of the spectrum. As $\tilde{r} \rightarrow 0$, the location of the phase transition approaches the expected BPP value.

Notably, the full-rank ($\tilde{r} \rightarrow 1$) limit can be treated similarly to the $\tilde{r} \rightarrow 0$ limit. Equation (8) splits into bulk and outlier contributions, now with the noise-disturbed signal producing the bulk and the noise leading to delta function peaks. A short computation – described in the Appendix – leads to the following expression for the $1 - \tilde{r}$ smallest eigenvalues:

$$x_0 = \begin{cases} \sigma^2 \left(1 - \frac{1}{\mathcal{A}}\right) \left(1 - \frac{\sigma^2}{\mathcal{A}} \frac{1}{\vartheta^2}\right), & \vartheta^2 > \frac{\sigma^2}{\mathcal{A}} (1 + \sqrt{\mathcal{A} - 1}) \\ \sigma^2 \left(1 - \frac{1}{\mathcal{A}}\right) \frac{\sqrt{\mathcal{A} - 1}}{1 + \sqrt{\mathcal{A} - 1}}, & \text{else.} \end{cases} \quad (12)$$

We refer to this as the “analog BPP” phase transition, marked by a black dot in Fig. 2.

Large Signals: In many applications the signal is large compared to the noise, and it is convenient to describe the two components of our distribution – the noise bulk and signal bulk – independently using an asymptotic ap-

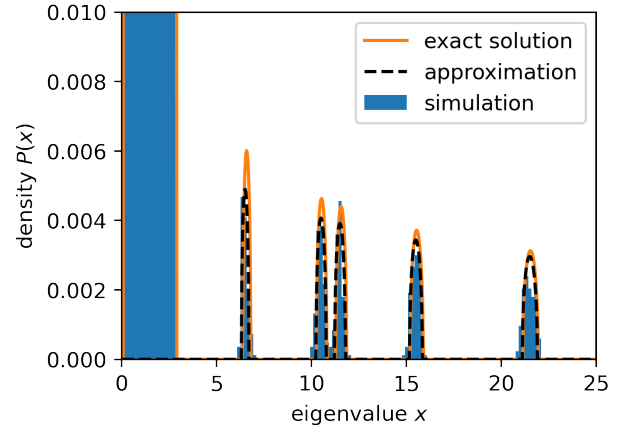


FIG. 5. Spectral density for five distinct signals $\{\vartheta_i^2\}_{i=1,\dots,5} = \{5, 9, 10, 14, 20\}$, each degenerate with a rank ratio $\tilde{r}_i = 1/500$. The exact solution is determined numerically via recursion of Eq. (15), as an approximate solution we add up the asymptotic density (14) for each signal separately, and the histogram stems from numerical simulations. We conduct 100 runs for a finite $p \times q$ dim. matrix with $q = 500$, $p = \mathcal{A}q$, and $\mathcal{A} = 2$.

proximation to Eq. (11). In particular, when $\vartheta^2 \gg \sigma^2$ we expect the signal to be concentrated around values of $z = \theta^2 + \mathcal{O}(1)$ with $|z| \gg \sigma^2$. Expanding (11) in powers of $1/z$, and using $G_-^{\text{MP}}(z) = z^{-1} + \mathcal{O}(z^{-2})$ and $G_+^{\text{MP}}(z) = \mathcal{A}\sigma^{-2} - \mathcal{A}z^{-1} + \mathcal{O}(z^{-2})$, yields a quadratic equation for G when terms of order $\mathcal{O}(z^{-1})$ are neglected. The two solutions are

$$G_{\pm}^{\text{aprx}}(z) = \frac{\alpha(z) \pm \sqrt{\alpha^2(z) - \frac{8\sigma^2}{\mathcal{A}}(\alpha(z) + \tilde{r}\vartheta^2 - 2\sigma^2/\mathcal{A})}}{4z\sigma^2/\mathcal{A}} \quad (13)$$

with $\alpha(z) := z - \vartheta^2 - \sigma^2(1 - 3/\mathcal{A})$ and where G_-^{aprx} corresponds to the non-negative eigenvalue density

$$P^{\text{aprx}}(x) = \frac{\mathcal{A}}{4\pi x \sigma^2} \left\{ [x - \vartheta^2 - \sigma^2(1 - 3/\mathcal{A})]^2 - \frac{8\sigma^2}{\mathcal{A}} \left[x - (1 - \tilde{r})\vartheta^2 - \sigma^2(1 - 1/\mathcal{A}) \right] \right\}^{1/2} \quad (14)$$

This is an approximate formula for the outlier (i.e. signal) bulk, valid in the large θ limit. This expression, somewhat similar to the Marchenko-Pastur law, demonstrates that even in the large signal limit the noise term effectively broadens the distribution of signal eigenvalues. The accuracy of this approximation at large signal is demonstrated in Fig. 4, where it is compared both to the exact solution from the fourth-order polynomial and to numerical simulations.

Arbitrary Signal Matrices: Most applications exhibit not a single degenerate signal but many distinct signals.

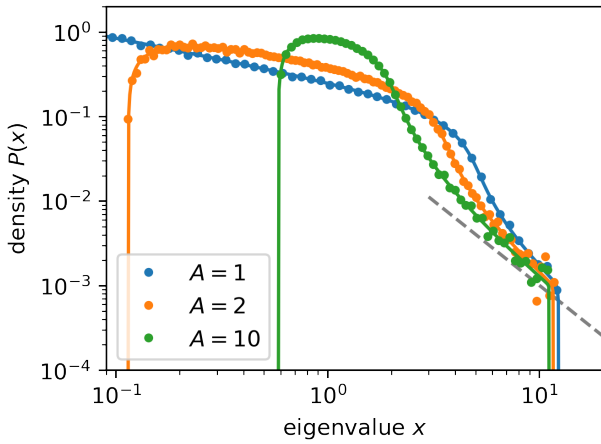


FIG. 6. Theoretical predictions via Eq. (38) and numerical simulations with signal eigenvalues distributed according to an inverse square power law between $k = 0.1$ and $K = 10$. We conduct 100 runs for a finite $p \times q$ dim. matrix with $q = 1000$, $p = \mathcal{A}q$. The dashed line is proportional to x^{-2} .

In this case solving (8) becomes more complicated. For example, if the signal matrix has n distinct eigenvalues, each of which has an eigenspace with rank that scales linearly with q , then (8) is a polynomial equation of order $2n + 2$. More generally, for arbitrary signal matrices we have

$$G(z) = \int_0^{+\infty} \frac{\rho_0(\vartheta^2) d(\vartheta^2)}{z[1 - \frac{\sigma^2}{\mathcal{A}} G(z)] - \sigma^2(1 - \frac{1}{\mathcal{A}}) - \frac{\vartheta^2}{1 - \frac{\sigma^2}{\mathcal{A}} G(z)}} \quad (15)$$

where ρ_0 is the eigenvalue density of $W_0^\top W_0$. This relation reproduces the result by Dozier and Silverstein ([26]), where $g(z) = (1 - 1/\mathcal{A})/z + G(z)/\mathcal{A}$ is used as a Green function, $\varrho_0(\vartheta^2) = (1 - 1/\mathcal{A})\delta(\vartheta^2) + \rho_0(\vartheta^2)/\mathcal{A}$ as a signal eigenvalue density, and $\sigma^2/q = \mathcal{A}\sigma^2/p$ in the second moments.

In many applications, such as neural networks, the signals may make up a non-negligible portion of the total rank. In the large q limit, these signals may either cluster around a finite number of values (in which case we would obtain a finite order polynomial equation for $G(z)$) or they may form a continuous distribution (in which case we would need to use the more general integral equation).

An example is shown in Fig. 5 in the case where we have five distinct signal eigenvalues, each with non-vanishing rank ratio. As before, we compare the exact solution, an approximation, and numerical simulations all of which match well. The exact solution is determined via Eq. (15), where ρ_0 is a sum of delta peaks and equal weights. This gives an order 12 polynomial which can be written as a fixed-point equation and solved iteratively.

Shouldering signals are approximated as large distinct signals almost without error, as in the previous section.

Another example, perhaps more useful for applications, is a full-rank signal matrix whose singular value distribution exhibits a power law. Assuming $\rho_0(x) \sim x^{-2}$, the integral in Eq. (15) is solvable exactly, see Appendix, and its Green function can be determined numerically. In Fig. 6 we depict the predicted eigenvalue densities and numerical simulations which again show excellent agreement.

Discussion: In this paper, we investigated the BBP-type phase transition for an extensive number of signals in a signal-plus-noise matrix setup. Utilizing methods from Random Matrix Theory such as the replica method, we established a framework to explore the transition from low-rank signals to full-rank signals. We demonstrated the spectral density's splitting behavior into two distinct bulks through a phase diagram, presented a new scaling law in the low-rank regime, and showcased the practicality of an approximation of the density's outlier part for multiple distinct signals.

The authors gratefully acknowledge useful conversations with B. Ménard. This work was performed in part at the Aspen Center for Physics, which is supported by National Science Foundation grant PHY-2210452. The work of A.M. and B.R. is supported in part by the Simons Foundation Grant No. 12574. Research of A.M. is supported in part by the Natural Sciences and Engineering Research Council of Canada (NSERC), funding reference number SAPIN/00047-2020. B.R. would like to acknowledge support by DFG grant RO/2247/16-1.

- [1] J. S. Bendat and A. G. Piersol, *Random Data: Analysis and Measurement Procedures* (Wiley, 2010).
- [2] E. P. Wigner, Characteristic vectors of bordered matrices with infinite dimensions, *Annals of Mathematics* **62**, 548 (1955).
- [3] E. P. Wigner, On the distribution of the roots of certain symmetric matrices, *Annals of Mathematics* **67**, 325 (1958).
- [4] H. E. Stanley, P. Gopikrishnan, V. Plerou, and L. A. N. Amaral, Quantifying fluctuations in economic systems by adapting methods of statistical physics, *Physica A: Statistical Mechanics and its Applications* **287**, 339 (2000).
- [5] L. Laloux, P. Cizeau, J.-P. Bouchaud, and M. Potters, Noise dressing of financial correlation matrices, *Physical Review Letters* **83**, 1467 (1999).
- [6] T. Guhr, A. Müller-Groeling, and H. A. Weidenmüller, Random-matrix theories in quantum physics: common concepts, *Physics Reports* **299**, 189 (1998).
- [7] J. L. Olesen, A. Ianus, L. Østergaard, N. Shemesh, and S. N. Jespersen, Tensor denoising of multidimensional mri data, *Magnetic Resonance in Medicine* **89**, 1160 (2023).
- [8] A. M. Sengupta and P. P. Mitra, Capacity of multivariate channels with multiplicative noise: I. random matrix techniques and large- n expansions for full transfer matrices (2000), arXiv:physics/0010081 [physics.data-an].

[9] A. K. Lampinen and S. Ganguli, An analytic theory of generalization dynamics and transfer learning in deep linear networks (2019), arXiv:1809.10374 [stat.ML].

[10] Z. D. Bai, Methodologies in spectral analysis of large dimensional random matrices, a review, *Statistica Sinica* **9**, 611 (1999).

[11] J. Bun, J.-P. Bouchaud, and M. Potters, Cleaning large correlation matrices: Tools from random matrix theory, *Physics Reports* **666**, 1 (2017).

[12] F. Benaych-Georges and R. R. Nadakuditi, The singular values and vectors of low rank perturbations of large rectangular random matrices, *Journal of Multivariate Analysis* **11**, 120 (2012).

[13] T. Tao, Outliers in the spectrum of iid matrices with bounded rank perturbations, *Probability Theory and Related Fields* **155**, 231 (2013).

[14] Z. D. Bai and J. W. Silverstein, No eigenvalues outside the support of the limiting spectral distribution of large-dimensional sample covariance matrices, *The Annals of Probability* **26**, 316 (1998).

[15] J. Baik, G. Ben Arous, and S. Péché, Phase transition of the largest eigenvalue for nonnull complex sample covariance matrices, *The Annals of Probability* **33**, 1643 (2005).

[16] S. Péché, The largest eigenvalue of small rank perturbations of hermitian random matrices (2005), arXiv:math/0411487 [math.PR].

[17] I. D. Landau, G. C. Mel, and S. Ganguli, Singular vectors of sums of rectangular random matrices and optimal estimation of high-rank signals: The extensive spike model, *Physical Review E* **108**, 10.1103/physreve.108.054129 (2023).

[18] F. Pourkamali and N. Macris, Rectangular rotational invariant estimator for general additive noise matrices (2023), arXiv:2304.12264 [cs.IT].

[19] E. Troiani, V. Erba, F. KRZAKALA, A. Maillard, and L. Zdeborová, Optimal denoising of rotationally invariant rectangular matrices (2022).

[20] J. Barbier and N. Macris, Statistical limits of dictionary learning: Random matrix theory and the spectral replica method, *Phys. Rev. E* **106**, 024136 (2022).

[21] A. Maillard, F. Krzakala, M. Mézard, and L. Zdeborová, Perturbative construction of mean-field equations in extensive-rank matrix factorization and denoising, *Journal of Statistical Mechanics: Theory and Experiment* **2022**, 083301 (2022).

[22] P. Fleig and I. Nemenman, Statistical properties of large data sets with linear latent features, *Phys. Rev. E* **106**, 014102 (2022).

[23] A. M. Sengupta and P. P. Mitra, Distributions of singular values for some random matrices, *Physical Review E* **60**, 3389 (1999).

[24] D. C. Hoyle and M. Rattray, Limiting form of the sample covariance eigenspectrum in pca and kernel pca, in *Advances in Neural Information Processing Systems*, Vol. 16, edited by S. Thrun, L. Saul, and B. Schölkopf (MIT Press, 2003).

[25] D. C. Hoyle and M. Rattray, Principal-component-analysis eigenvalue spectra from data with symmetry-breaking structure, *Physical Review E* **69**, 10.1103/PhysRevE.69.026124 (2004).

[26] R. B. Dozier and J. W. Silverstein, On the empirical distribution of eigenvalues of large dimensional information-plus-noise-type matrices, *Journal of Multivariate Analysis* **98**, 678 (2007).

[27] R. P. Mondaini and S. C. de Albuquerque Neto, Revisiting the evaluation of a multidimensional gaussian integral, *Journal of Applied Mathematics and Physics* , 449 (2017).

[28] K. G. Brock, How rare are singular matrices?, *The Mathematical Gazette* **89**, 378 (2005).

[29] R. S. Irving, *Integers, Polynomials, and Rings: A Course in Algebra*, Undergraduate Texts in Mathematics (Springer Science & Business Media, 2004).

Details on the Replica Method In the quantity $Z^n(z)$, we introduce new integration variables via inclusion of unity through Gaussian integrals. With a change of variables we get rid of the quadratic terms in W . Afterwards, we take the average w.r.t. M and conduct a Hubbard-Stratonovich transformation,

$$\begin{aligned} \langle Z^n(z) \rangle_M &= \left(\frac{q}{2\pi} \right)^{n(p+q)/2} \int_{\mathbb{R}^{n(p+q)}} \prod_{\alpha=1}^n \mathcal{D}X_\alpha \mathcal{D}Y_\alpha \\ &\times e^{-\frac{q}{2} \sum_{\alpha=1}^n (X_\alpha^\top z X_\alpha + Y_\alpha^\top Y_\alpha + Y_\alpha^\top W_0 X_\alpha + (W_0 X_\alpha)^\top Y_\alpha)} \\ &\times e^{\frac{q}{2} \frac{\sigma^2}{\mathcal{A}} \text{Tr} \sum_{\alpha, \beta=1}^n X_\alpha Y_\alpha^\top Y_\beta X_\beta^\top} \cdot \frac{1}{(2\pi)^{pq/2}} \\ &\times \int_{\mathbb{R}^{pq}} \mathcal{D}M \exp \left\{ -\frac{p}{2\sigma^2} \text{Tr} \left[\left(M + \frac{\sigma^2}{\mathcal{A}} \sum_{\alpha=1}^n Y_\alpha X_\alpha^\top \right)^\top \right. \right. \\ &\left. \left. \times \left(M + \frac{\sigma^2}{\mathcal{A}} \sum_{\alpha=1}^n Y_\alpha X_\alpha^\top \right) \right] \right\}. \end{aligned} \quad (16)$$

The average can be readily performed. Regarding the quartic terms $X_\beta^\top X_\alpha Y_\alpha^\top Y_\beta$, we insert unity through a product of delta distributions in their integral representation. Herein, we replace $X_\beta^\top X_\alpha$ by $Q_{\alpha\beta}$ for every $\alpha, \beta \in \{1, \dots, n\}$. The previous variables are integrated away via a combined high-dimensional Gaussian integral with a matrix A in its quadratic form:

$$\langle Z^n(z) \rangle_M = \left(\frac{q}{4\pi} \right)^{n^2} \int_{\mathbb{R}^{2n^2}} \mathcal{D}Q \mathcal{D}R e^{-\frac{q}{2} [\text{Tr}(iRQ) + \frac{1}{q} \text{Tr} \ln A_+]} \quad (17)$$

where A_+ is the symmetrized version $A_+ := (A + A^\top)/2$ ([27]) of A , which is defined below. The Gaussian integral could be evaluated because singular matrices have Lebesgue measure zero, i.e. $\det A_+ \neq 0$ almost surely ([28]). It is convenient to label the matrix A using the indices α, β , therewith it is defined as

$$A_{\alpha\beta} := \begin{pmatrix} (z\delta_{\alpha\beta} - iR_{\alpha\beta})\mathbf{1}_q & \delta_{\alpha\beta}W_0^\top \\ \delta_{\alpha\beta}W_0 & (\delta_{\alpha\beta} - \frac{\sigma^2}{\mathcal{A}}Q_{\alpha\beta})\mathbf{1}_p \end{pmatrix}. \quad (18)$$

Observe how each entry is a matrix of dimension $p + q$ itself so that the exponent in Eq. (17) indeed scales with q in total. Now, we apply a saddle-point approximation for Eq. (17) and choose a replica-diagonal ansatz letting $Q_{\alpha\beta} = \delta_{\alpha\beta}Q(z)$ and $R_{\alpha\beta} = -i\delta_{\alpha\beta}\mathcal{R}(z)$. Only the

highest-order term $\langle Z^n(z) \rangle_M \sim e^{-\frac{nq}{2}\mathcal{S}(z, \mathcal{Q}(z), \mathcal{R}(z))}$ survives the analytic continuation. The maximizing exponent contains the self-energy

$$\begin{aligned} \mathcal{S}(z, \mathcal{Q}(z), \mathcal{R}(z)) &= \mathcal{R}(z)\mathcal{Q}(z) + \mathcal{A} \ln \left(1 - \frac{\sigma^2}{\mathcal{A}} \mathcal{Q}(z) \right) \\ &+ \frac{1}{q} \text{Tr} \ln \left([z - \mathcal{R}(z)]\mathbb{1}_q - \frac{W_0^\top W_0}{\mathbb{1}_p - \frac{\sigma^2}{\mathcal{A}} \mathcal{Q}(z)} \right) \end{aligned} \quad (19)$$

which uses the Schur complement to rewrite the determinant of a matrix such as $A_{\alpha\beta}$. The saddle-point equations are given by $\partial_Q \mathcal{S} = 0$, $\partial_R \mathcal{S} = 0$. They are quite similar and allow for a simple relation between $\mathcal{Q}(z)$ and $\mathcal{R}(z)$. Then, a full description is given by

$$\mathcal{Q}(z) = \frac{1}{z - \mathcal{R}(z)} \left(1 + \frac{1}{q} \sum_{i=1}^r \frac{\vartheta_i^2}{[1 - \frac{\sigma^2}{\mathcal{A}} \mathcal{Q}(z)][z - \mathcal{R}(z)] - \vartheta_i^2} \right) \quad (20)$$

and

$$\frac{\mathcal{R}(z)}{z\sigma^2} = \frac{1 - 1/\mathcal{A}}{z} + \frac{\mathcal{Q}(z)}{\mathcal{A}}. \quad (21)$$

Moreover, observing $\partial_R \mathcal{S} = \mathcal{Q}(z) - \partial_z \mathcal{S}$, the Green function is found to be

$$G(z) = \lim_{q \rightarrow +\infty} \partial_z \mathcal{S}(z, \mathcal{Q}(z), \mathcal{R}(z)) \quad (22)$$

such that $\mathcal{Q}(z)$ is related to the Green function via $G(z) = \lim_{q \rightarrow +\infty} \mathcal{Q}(z)$.

Details on the Analytic Green Function Solution
Eq. (11) is a fourth-order polynomial with a few algebraic manipulations:

$$\begin{aligned} 0 &= z^2 \frac{\sigma^6}{\mathcal{A}^3} G(z)^4 + \frac{\sigma^4}{\mathcal{A}^2} \left[2z\sigma^2 \left(1 - \frac{1}{\mathcal{A}} \right) - 3z^2 \right] G(z)^3 \\ &+ \frac{\sigma^2}{\mathcal{A}} \left[3z^2 - z\vartheta^2 + \sigma^4 \left(1 - \frac{1}{\mathcal{A}} \right)^2 - 4z\sigma^2 \left(1 - \frac{1}{\mathcal{A}} \right) \right. \\ &\left. + z \frac{\sigma^2}{\mathcal{A}} \right] G(z)^2 + \left[z\vartheta^2 - \vartheta^2\sigma^2 \left(1 - \frac{1}{\mathcal{A}} \right) \right. \\ &\left. + 2z\sigma^2 \left(1 - \frac{1}{\mathcal{A}} \right) - \sigma^4 \left(1 - \frac{1}{\mathcal{A}} \right)^2 - z^2 \right. \\ &\left. + \frac{\sigma^4}{\mathcal{A}} \left(1 - \frac{1}{\mathcal{A}} \right) - 2z \frac{\sigma^2}{\mathcal{A}} \right] G(z) \\ &+ z - \sigma^2 \left(1 - \frac{1}{\mathcal{A}} \right) - (1 - \tilde{r})\vartheta^2. \end{aligned} \quad (23)$$

This representation is only worthwhile for non-zero \tilde{r} . Let us shorten the notation and identify the polynomial with

$$0 = A(z)G^4(z) + B(z)G^3(z) + C(z)G^2(z) + D(z)G(z) + E(z). \quad (24)$$

The full solution reads:

$$\begin{aligned} G_{1,\dots,4}(z) &= -\frac{B(z)}{4A(z)} \mp_{(I)} \frac{1}{2} \sqrt{2y - a} \\ &\pm_{(II)} \frac{1}{2} \sqrt{-2y - a \pm_{(I)} \frac{2b}{\sqrt{2y - a}}} \end{aligned} \quad (25)$$

where $\pm_{(I)}$ and $\pm_{(II)}$ are unrelated signs so as to give four sign combinations in total,

$$\begin{aligned} y = y(z) &:= \frac{a}{6} + \sqrt[3]{-\frac{n}{2} + \sqrt{\frac{n^2}{4} + \frac{m^3}{27}}} \\ &- \frac{m}{3} \sqrt[3]{-\frac{n}{2} + \sqrt{\frac{n^2}{4} + \frac{m^3}{27}}} \end{aligned} \quad (26a)$$

$$m = m(z) := -\left(\frac{a^2(z)}{12} + c(z) \right), \quad (26b)$$

$$n = n(z) := -\frac{a^3(z)}{108} + \frac{a(z)c(z)}{3} - \frac{b^2(z)}{8} \quad (26c)$$

and

$$a(z) := -\frac{3B^2(z)}{8A^2(z)} + \frac{C(z)}{A(z)}, \quad (27a)$$

$$b(z) := \frac{B^3(z)}{8A^3(z)} - \frac{B(z)C(z)}{2A^2(z)} + \frac{D(z)}{A(z)} \quad (27b)$$

$$c(z) := -\frac{3B^4(z)}{256A^4(z)} + \frac{C(z)B^2(z)}{16A^3(z)} - \frac{B(z)D(z)}{4A^2(z)} + \frac{E(z)}{A(z)}. \quad (27c)$$

The polynomial gives rise to the discriminant $\Delta = \Delta(z)$ defined by ([29])

$$\begin{aligned} \Delta &:= 256A^3(z)E^3(z) - 192A^2(z)B(z)D(z)E^2(z) \\ &- 128A^2(z)C^2(z)E^2(z) + 144A^2(z)C(z)D^2(z)E(z) \\ &- 27A^2(z)D^4(z) + 144A(z)B^2(z)C(z)E^2(z) \\ &- 6A(z)B^2(z)D^2(z)E(z) - 80A(z)B(z)C^2(z)D(z)E(z) \\ &+ 18A(z)B(z)C(z)D^3(z) + 16A(z)C^4(z)E(z) \\ &- 4A(z)C^3(z)D^2(z) - 27B^4(z)E^2(z) \\ &+ 18B^3(z)C(z)D(z)E(z) - 4B^3(z)D^3(z) \\ &- 4B^2(z)C^3(z)E(z) + B^2(z)C^2(z)D^2(z). \end{aligned} \quad (28)$$

The discriminant's roots are responsible for the spectrum's boundaries, because they mark a change in the number of real and imaginary solutions. We can furthermore relate the discriminant to one radicand in our full Green function expression:

$$\frac{n^2(z)}{4} + \frac{m^3(z)}{27} = -\frac{27}{4 \cdot [6A(z)]^6} \Delta(z). \quad (29)$$

The left-hand side is more suitable for the numerical determination of roots due to its smaller scale, leading to fewer fluctuations near zero.

Details on the Full-Rank Limit The full-rank limit can be dealt with similarly to the low-rank approximation. The self-consistency equation (8) may be split into a major contribution

$$G(z) = \frac{1}{z[1 - \frac{\sigma^2}{\mathcal{A}} G(z)] - \sigma^2(1 - 1/\mathcal{A}) - \frac{\vartheta^2}{1 - \frac{\sigma^2}{\mathcal{A}} G(z)}} \quad (30)$$

which is now containing the signal, and a minor contribution from the noise-only part

$$0 = z \left[1 - \frac{\sigma^2}{\mathcal{A}} G(z) \right] - \sigma^2(1 - 1/\mathcal{A}) \quad (31)$$

responsible for exceptions to the rule – the outliers. They can be determined without explicit knowledge of the Green function. The Blue function, the functional inverse of G , can be used instead. Let us denote it by B_{fr} in this full-rank case. Eq. (31) is then equivalent to

$$G(z) = \frac{1}{\frac{\sigma^2}{\mathcal{A}} - \vartheta^2} \iff z = B_{\text{fr}} \left(\frac{1}{\frac{\sigma^2}{\mathcal{A}} - \vartheta^2} \right) \quad (32)$$

Additionally, Eq. (30) yields the explicit form of B_{fr} via $z = B_{\text{fr}}(G(z))$:

$$B_{\text{fr}}(y) = \frac{1}{1 - \frac{\sigma^2}{\mathcal{A}} y} \left(\frac{1}{y} + \sigma^2(1 - 1/\mathcal{A}) + \frac{\vartheta^2}{1 - \frac{\sigma^2}{\mathcal{A}} y} \right). \quad (33)$$

The spectrum's boundaries are characterized by infinite slopes, hence any y with $B'_{\text{fr}}(y) = 0$ yields a boundary $B(y)$. Inserting $y = (\sigma^2/\mathcal{A} - \vartheta^2)^{-1}$ from Eq. (32) into $B'_{\text{fr}}(y) = 0$ reveals a value for the critical signal at which the outlier is exactly at a boundary.

$$\vartheta_{\text{crit}}^2 = \frac{\sigma^2}{\mathcal{A}} \left(1 + \sqrt{\mathcal{A} - 1} \right). \quad (34)$$

It is, in fact, the lower boundary, because larger signals shift the major bulk away, giving rise to separate delta peaks from the noise-only contribution. They are described via a case distinction not unlike the BBP phase

transition

$$x_0 = \begin{cases} \sigma^2(1 - 1/\mathcal{A})(1 - \frac{\sigma^2}{\mathcal{A}} \frac{1}{\vartheta^2}) & , \quad \vartheta^2 > \frac{\sigma^2}{\mathcal{A}}(1 + \sqrt{\mathcal{A} - 1}) \\ \sigma^2(1 - 1/\mathcal{A}) \frac{\sqrt{\mathcal{A} - 1}}{1 + \sqrt{\mathcal{A} - 1}} & , \quad \text{else.} \end{cases} \quad (35)$$

only now with every of the $q - r \ll q$ noise-only eigenvalues at a common value.

Details on Large Signals Following the instructions stated in the main text, the series expansion of Eq. (11) in powers of z^{-1} reads

$$\begin{aligned} 0 = z^2 G^2(z) & \left[-\frac{2\sigma^2}{\mathcal{A}} - \frac{\sigma^2}{\mathcal{A}} \frac{z - \vartheta^2}{z} \right] \\ & + zG(z) \left[\alpha(z) - \sigma^2(1 - 1/\mathcal{A}) \frac{z - \vartheta^2}{z} \right] \\ & - \left[\alpha(z) + \tilde{r}\vartheta^2 - \frac{2\sigma^2}{\mathcal{A}} - \sigma^2 \frac{z - \vartheta^2}{z} \right] + \mathcal{O}(z^{-1}) \end{aligned} \quad (36)$$

where $\alpha(z) = z - \vartheta^2 - \sigma^2(1 - 3/\mathcal{A})$. With the assumption $z - \vartheta^2 = \mathcal{O}(1)$ we confine the validity of the expansion, but three more terms are negligible. Excluding all but the highest two orders yields

$$0 = -\frac{2\sigma^2}{\mathcal{A}} z^2 G^2(z) + \alpha(z)zG(z) - \left[\alpha(z) + \tilde{r}\vartheta^2 - \frac{2\sigma^2}{\mathcal{A}} \right]. \quad (37)$$

Power Law Distributed Signals Assuming a full-rank signal matrix W_0 with the eigenvalues of $W_0^\top W_0$ following an inverse square power law, $\rho_0(x) = (1/k - 1/K)^{-1}x^{-2}$ for $x \in (k, K)$ and zero otherwise, the self-consistency equation (15) becomes

$$\begin{aligned} G(z) = & \left[-1 + \frac{1}{\frac{1}{k} - \frac{1}{K}} \frac{1}{C(z, G)} \log \left(\frac{1 - \frac{C(z, G)}{k}}{1 - \frac{C(z, G)}{K}} \right) \right] \\ & \times \frac{1}{1 - \frac{\sigma^2}{\mathcal{A}} G(z)} \frac{1}{C(z, G)} \end{aligned} \quad (38)$$

where $C(z, G) = [1 - \frac{\sigma^2}{\mathcal{A}} G(z)](z[1 - \frac{\sigma^2}{\mathcal{A}} G(z)] - \sigma^2(1 - 1/\mathcal{A}))$.